time-dependent Fourier transform might correspond to reflections from a fin on the rocket that is alternately moving toward and then away from the antenna because of the spinning of the rocket. Figure 10.19(b) shows an estimate of the Doppler frequency as a function of time. This estimate was obtained simply by locating the highest peak in each DFT.

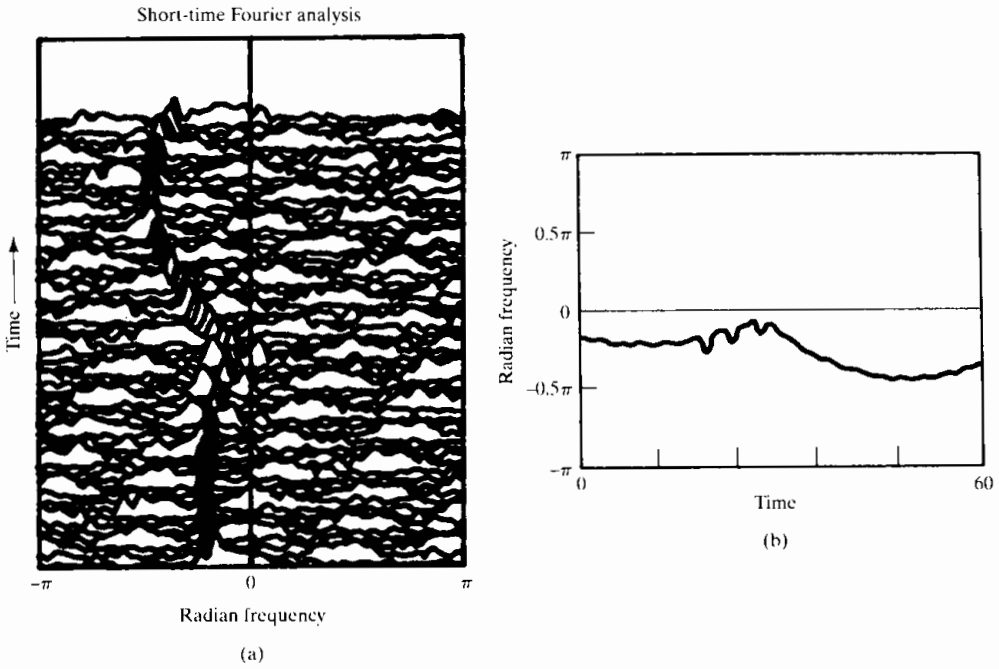

Figure 10.19 Illustration of time-dependent Fourier analysis of Doppler radar signal. (a) Sequence of Fourier transforms of Doppler radar signal. (b) Doppler frequency estimated by picking the largest peak in the time-dependent Fourier transform.

10.6 FOURIER ANALYSIS OF STATIONARY RANDOM SIGNALS: THE PERIODOGRAM

In the previous sections, we discussed and illustrated Fourier analysis for sinusoidal signals with stationary (non-time-varying) parameters and for nonstationary signals such as speech and radar. In cases where the signal can be modeled by a sum of sinusoids or a linear system excited by a periodic pulse train, the Fourier transforms of finite-length segments of the signal have a convenient and natural interpretation in terms of Fourier transforms, windowing, and linear system theory. However, more noiselike signals, such as the example of unvoiced speech in Section 10.5.1, are best modeled as random signals.

As we discussed in Section 2.10 and as shown in Appendix A, random processes are often used to model signals when the process that generates the signal is too complex for a reasonable deterministic model. Typically, when the input to a linear time-invariant system is modeled as a stationary random process, many of the essential characteristics of the input and output are adequately represented by averages, such as the mean value (dc level), variance (average power), autocorrelation function, or power density

spectrum. Consequently, it is of particular interest to estimate these for a given signal. As discussed in Appendix A, a typical estimate of the mean value of a stationary random process from a finite-length segment of data is the *sample mean*, defined as

$$\hat{m}_x = \frac{1}{L}\sum_{n=0}^{L-1} x[n]. \tag{10.48}$$

Similarly, a typical estimate of the variance is the *sample variance*, defined as

$$\hat{\sigma}_x^2 = \frac{1}{L}\sum_{n=0}^{L-1}(x[n] - \hat{m}_x)^2. \tag{10.49}$$

The sample mean and the sample variance, which are themselves random variables, are *unbiased* and *asymptotically unbiased* estimators, respectively; i.e., the expected value of $\hat{m}_x$ is the true mean m_x and the expected value of $\hat{\sigma}_x^2$ approaches the true variance σ_x^2 as L approaches ∞. Furthermore, they are both *consistent* estimators; i.e., they improve with increasing L, since their variances approach zero as L approaches ∞.

In the remainder of this chapter, we study the estimation of the power spectrum[5] of a random signal using the DFT. As we will see, there are two basic approaches to estimating the power spectrum. One approach, which we develop in this section, is referred to as *periodogram analysis* and is based on direct Fourier transformation of finite-length segments of the signal. The second approach, developed in Section 10.7, is to first estimate the autocovariance sequence and then compute the Fourier transform of this estimate. In either case, we are typically interested in obtaining unbiased consistent estimators. Unfortunately, the analysis of such estimators is very difficult, and generally, only approximate analyses can be accomplished. Even approximate analyses are beyond the scope of this text, and we refer to the results of such analyses only in a qualitative way. Detailed discussions are given in Blackman and Tukey (1958), Hannan (1960), Jenkins and Watts (1968), Koopmans (1995), Kay and Marple (1981), Marple (1987), and Kay (1988).

10.6.1 The Periodogram

Let us consider the problem of estimating the power density spectrum $P_{ss}(\Omega)$ of a continuous-time signal $s_c(t)$. An intuitive approach to the estimation of the power spectrum is suggested by Figure 10.1 and the associated discussion in Section 10.1; based on that approach, we now assume that the input signal $s_c(t)$ is a stationary random signal. The antialiasing lowpass filter creates a new stationary random signal whose power spectrum is bandlimited, so that the signal can be sampled without aliasing. Then $x[n]$ is a stationary discrete-time random signal whose power density spectrum $P_{xx}(\omega)$ is proportional to $P_{ss}(\Omega)$ over the bandwidth of the antialiasing filter; i.e.,

$$P_{xx}(\omega) = \frac{1}{T}P_{ss}\left(\frac{\omega}{T}\right), \qquad |\omega| < \pi, \tag{10.50}$$

where we have assumed that the cutoff frequency of the antialiasing filter is π/T and that T is the sampling period. (See Problem 10.33 for a further consideration of

[5]The term *power spectrum* is commonly used interchangeably with the more precise term *power density spectrum*.

sampling of random signals.) Consequently, a reasonable estimate of $P_{xx}(\omega)$ will provide a reasonable estimate of $P_{ss}(\Omega)$. The window $w[n]$ in Figure 10.1 selects a finite-length segment (L samples) of $x[n]$, which we denote $v[n]$, the Fourier transform of which is

$$V(e^{j\omega}) = \sum_{n=0}^{L-1} w[n]x[n]e^{-j\omega n}. \tag{10.51}$$

Consider as an estimate of the power spectrum the quantity

$$I(\omega) = \frac{1}{LU}|V(e^{j\omega})|^2, \tag{10.52}$$

where the constant U anticipates a need for normalization to remove bias in the spectral estimate. When the window $w[n]$ is the rectangular window sequence, this estimator for the power spectrum is called the *periodogram*. If the window is not rectangular, $I(\omega)$ is called the *modified periodogram*. Clearly, the periodogram has some of the basic properties of the power spectrum. It is nonnegative, and for real signals, it is a real and even function of frequency. Furthermore, it can be shown (Problem 10.26) that

$$I(\omega) = \frac{1}{LU} \sum_{m=-(L-1)}^{L-1} c_{vv}[m]e^{-j\omega m}, \tag{10.53}$$

where

$$c_{vv}[m] = \sum_{n=0}^{L-1} x[n]w[n]x[n+m]w[n+m]. \tag{10.54}$$

We note that the sequence $c_{vv}[m]$ is the aperiodic correlation sequence for the finite-length sequence $v[n] = w[n]x[n]$. Consequently, the periodogram is in fact the Fourier transform of the aperiodic correlation of the windowed data sequence.

Explicit computation of the periodogram can be carried out only at discrete frequencies. From Eqs. (10.51) and (10.52), we see that if the discrete-time Fourier transform of $w[n]x[n]$ is replaced by its DFT, we will obtain samples at the DFT frequencies $\omega_k = 2\pi k/N$ for $k = 0, 1, \ldots, N-1$. Specifically, samples of the periodogram are given by

$$I(\omega_k) = \frac{1}{LU}|V[k]|^2, \tag{10.55}$$

where $V[k]$ is the N-point DFT of $w[n]x[n]$. If we want to choose N to be greater than the window length L, appropriate zero-padding would be applied to the sequence $w[n]x[n]$.

If a random signal has a nonzero mean, its power spectrum has an impulse at zero frequency. If the mean is relatively large, this component will dominate the spectrum estimate, causing low-amplitude, low-frequency components to be obscured by leakage. Therefore, in practice the mean is often estimated using Eq. (10.48), and the resulting estimate is subtracted from the random signal before computing the power spectrum estimate. Although the sample mean is only an approximate estimate of the zero-frequency component, subtracting it from the signal often leads to better estimates at neighboring frequencies.

10.6.2 Properties of the Periodogram

The nature of the periodogram estimate of the power spectrum can be determined by recognizing that, for each value of ω, $I(\omega)$ is a random variable. By computing the mean and variance of $I(\omega)$, we can determine whether the estimate is biased and whether it is consistent.

From Eq. (10.53), the expected value of $I(\omega)$ is

$$\mathcal{E}\{I(\omega)\} = \frac{1}{LU} \sum_{m=-(L-1)}^{L-1} \mathcal{E}\{c_{vv}[m]\}e^{-j\omega m}. \tag{10.56}$$

The expected value of $c_{vv}[m]$ can be expressed as

$$\begin{aligned} \mathcal{E}\{c_{vv}[m]\} &= \sum_{n=0}^{L-1} \mathcal{E}\{x[n]w[n]x[n+m]w[n+m]\} \\ &= \sum_{n=0}^{L-1} w[n]w[n+m]\mathcal{E}\{x[n]x[n+m]\}. \end{aligned} \tag{10.57}$$

Since we are assuming that $x[n]$ is stationary,

$$\mathcal{E}\{x[n]x[n+m]\} = \phi_{xx}[m], \tag{10.58}$$

and Eq. (10.57) can then be rewritten as

$$\mathcal{E}\{c_{vv}[m]\} = c_{ww}[m]\phi_{xx}[m], \tag{10.59}$$

where $c_{ww}[m]$ is the aperiodic autocorrelation of the window, i.e.,

$$c_{ww}[m] = \sum_{n=0}^{L-1} w[n]w[n+m]. \tag{10.60}$$

From Eq. (10.56), Eq. (10.59), and the modulation–windowing property of Fourier transforms (Section 2.9.7), it follows that

$$\mathcal{E}\{I(\omega)\} = \frac{1}{2\pi LU} \int_{-\pi}^{\pi} P_{xx}(\theta)C_{ww}(e^{j(\omega-\theta)})d\theta, \tag{10.61}$$

where $C_{ww}(e^{j\omega})$ is the Fourier transform of the aperiodic autocorrelation of the window, i.e.,

$$C_{ww}(e^{j\omega}) = |W(e^{j\omega})|^2. \tag{10.62}$$

According to Eq. (10.61), the (modified) periodogram is a biased estimate of the power spectrum, since $\mathcal{E}\{I(\omega)\}$ is not equal to $P_{xx}(\omega)$. Indeed, we see that the bias arises as a result of convolution of the true power spectrum with the Fourier transform of the aperiodic autocorrelation of the data window. If we increase the window length, we expect that $W(e^{j\omega})$ should become more concentrated around $\omega = 0$, and thus $C_{ww}(e^{j\omega})$ should look increasingly like a periodic impulse train. If the scale factor $1/(LU)$ is correctly chosen, then $\mathcal{E}\{I(\omega)\}$ should approach $P_{xx}(\omega)$ as $W(e^{j\omega})$ approaches a periodic impulse train. The scale can be adjusted by choosing the normalizing constant U so that

$$\frac{1}{2\pi LU} \int_{-\pi}^{\pi} |W(e^{j\omega})|^2 d\omega = \frac{1}{LU} \sum_{n=0}^{L-1} (w[n])^2 = 1, \tag{10.63}$$

or

$$U = \frac{1}{L}\sum_{n=0}^{L-1}(w[n])^2. \tag{10.64}$$

For the rectangular window, we would then choose $U = 1$, while other data windows would require a value of $0 < U < 1$ if $w[n]$ is normalized to a maximum value of 1. Alternatively, the normalization can be absorbed into the amplitude of $w[n]$. Therefore, if properly normalized, the (modified) periodogram is asymptotically unbiased; i.e., the bias approaches zero as the window length increases.

To examine whether the periodogram is a consistent estimate or becomes a consistent estimate as the window length increases, it is necessary to consider the behavior of the variance of the periodogram. An expression for the variance of the periodogram is very difficult to obtain even in the simplest cases. However, it has been shown (see Jenkins and Watts, 1968) that over a wide range of conditions, as the window length increases,

$$\text{var}[I(\omega)] \simeq P_{xx}^2(\omega). \tag{10.65}$$

That is, the variance of the periodogram estimate is approximately the same size as the square of the power spectrum that we are estimating. Therefore, since the variance does not asymptotically approach zero with increasing window length, the periodogram is not a consistent estimate.

The properties of the periodogram estimate of the power spectrum just discussed are illustrated in Figure 10.20, which shows periodogram estimates of white noise using rectangular windows of lengths $L = 16, 64, 256$, and 1024. The sequence $x[n]$ was obtained from a pseudorandom-number generator whose output was scaled so that $|x[n]| \leq \sqrt{3}$. A good random-number generator produces a uniform distribution of amplitudes, and the sample-to-sample correlation is small. Thus, the power spectrum of the output of the random-number generator could be modeled in this case by $P_{xx}(\omega) = \sigma_x^2 = 1$ for all ω. For each of the four rectangular windows, the periodogram was computed with normalizing constant $U = 1$ and at frequencies $\omega_k = 2\pi k/N$ for

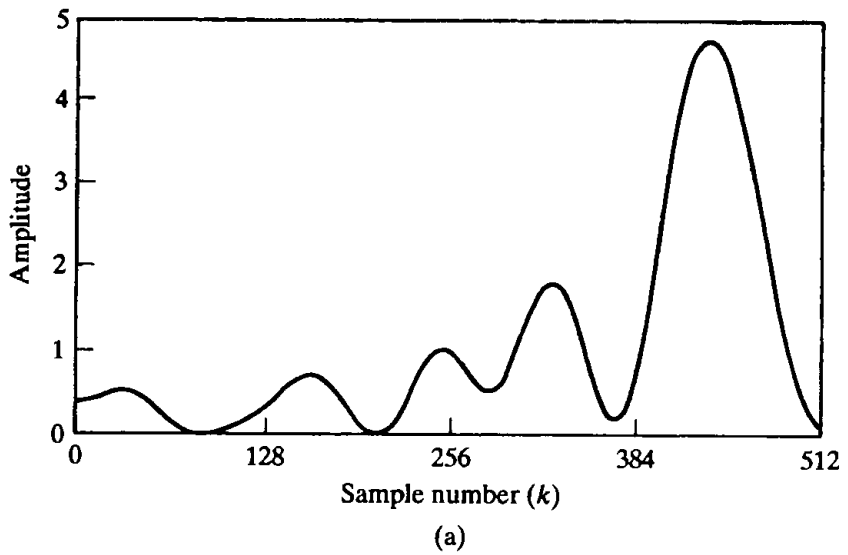

Figure 10.20 Periodograms of pseudorandom white-noise sequence. (a) Window length $L = 16$ and DFT length $N = 1024$.

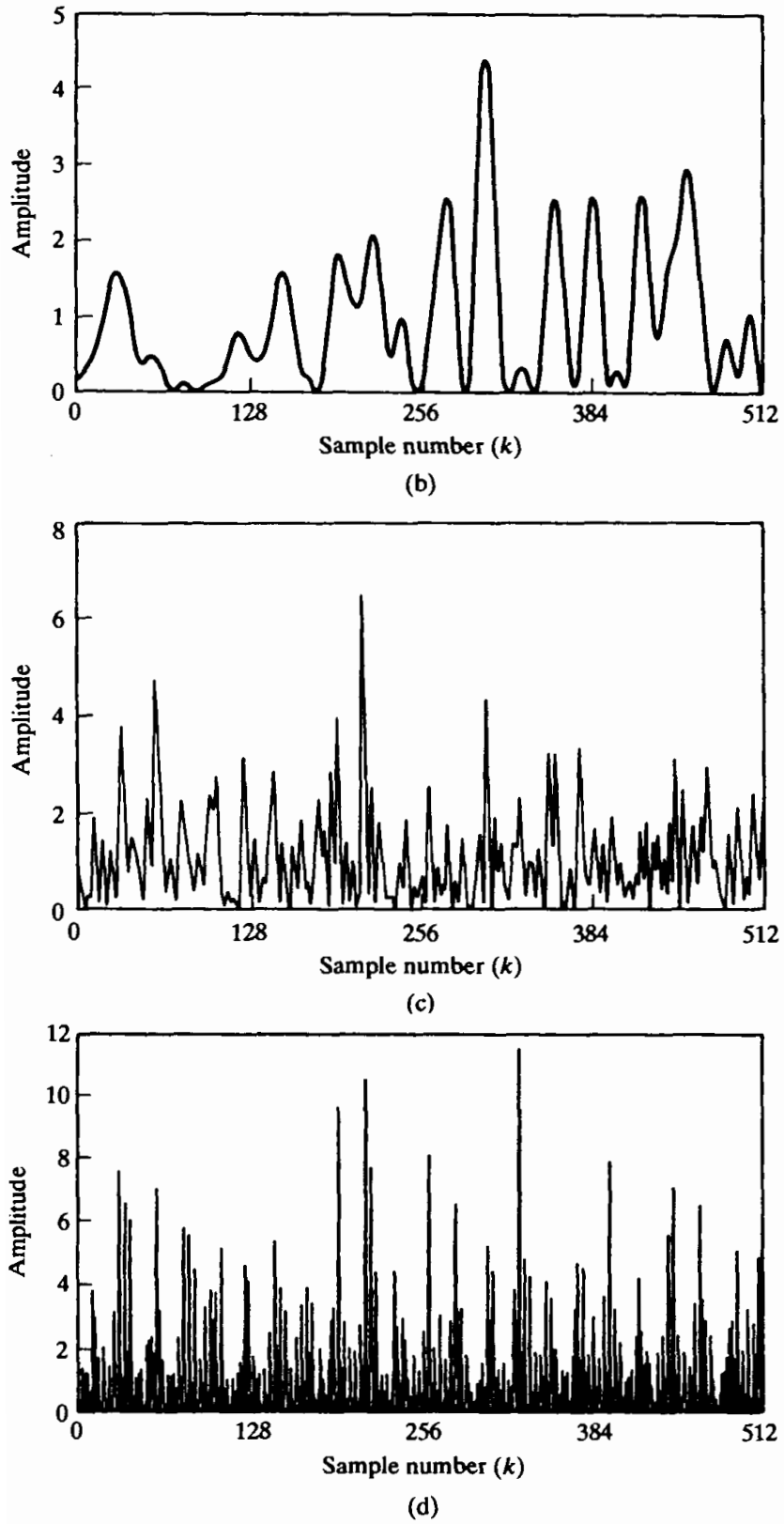

Figure 10.20 (*continued*) (b) $L = 64$ and $N = 1024$. (c) $L = 256$ and $N = 1024$. (d) $L = 1024$ and $N = 1024$.

$N = 1024$ using the DFT. That is,

$$I[k] = I(\omega_k) = \frac{1}{L}|V[k]|^2 = \frac{1}{L}\left|\sum_{n=0}^{L-1} w[n]x[n]e^{-j(2\pi/N)kn}\right|^2. \tag{10.66}$$

In Figure 10.20, the DFT values are connected by straight lines for purposes of display. Recall that $I(\omega)$ is real and an even function of ω so we only need to plot $I[k]$ for $0 \le k \le N/2$ corresponding to $0 \le \omega \le \pi$. We note that the spectral estimate fluctuates more rapidly as the window length L increases. This behavior can be understood by recalling that, although we view the periodogram method as a direct computation of the spectral estimate, we have seen that the underlying correlation estimate of Eq. (10.54) is, in effect, Fourier transformed to obtain the periodogram. Figure 10.21 illustrates a windowed sequence, $x[n]w[n]$, and a shifted version, $x[n+m]w[n+m]$, as required in Eq. (10.54). From this figure, we see that $L - m - 1$ signal values are involved in computing a particular correlation lag value $c_{vv}[m]$. Thus, when m is close to L, only a few values of $x[n]$ are involved in the computation, and we expect that the estimate of the correlation sequence will be considerably more inaccurate for these values of m and consequently will also show considerable variation between adjacent values of m. On the other hand, when m is small, many more samples are involved, and the variability of $c_{vv}[m]$ with m should not be as great. The variability at large values of m manifests itself in the Fourier transform as fluctuations at all frequencies, and thus, for large L, the periodogram estimate tends to vary rapidly with frequency. Indeed, it can be shown (see Jenkins and Watts, 1968) that if $N = L$, the periodogram estimates at the DFT frequencies $2\pi k/N$ become uncorrelated. Since, as N increases, the DFT frequencies get closer together, this behavior is inconsistent with our goal of obtaining a good estimate of the power spectrum. We would prefer to obtain a smooth spectrum

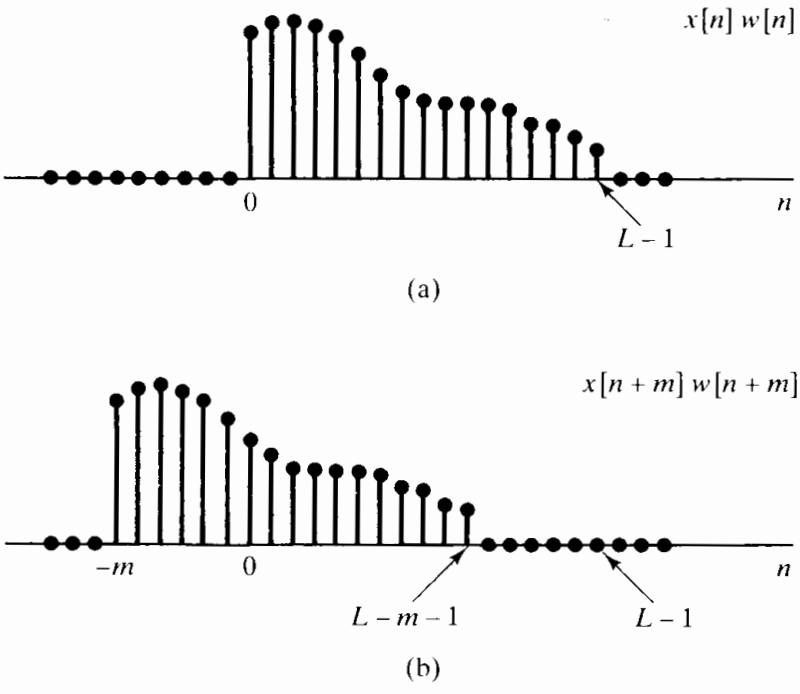

Figure 10.21 Illustration of sequences involved in Eq. (10.54). (a) A finite-length sequence. (b) Shifted sequence for $m > 0$.

estimate without random variations resulting from the estimation process. This can be accomplished by averaging multiple independent periodogram estimates to reduce the fluctuations.

10.6.3 Periodogram Averaging

The averaging of periodograms in spectrum estimation was first studied extensively by Bartlett (1953); later, after fast algorithms for computing the DFT were developed, Welch (1970) combined these computational algorithms with the use of a data window $w[n]$ to develop the method of averaging modified periodograms. In periodogram averaging, a data sequence $x[n], 0 \leq n \leq Q-1$, is divided into segments of length-L samples, with a window of length L applied to each; i.e., we form the segments

$$x_r[n] = x[rR + n]w[n], \qquad 0 \leq n \leq L-1. \tag{10.67}$$

If $R < L$ the segments overlap, and for $R = L$ the segments are contiguous. Note that Q denotes the length of the available data. The total number of segments depends on the values of, and relationship among, R, L, and Q. Specifically, there will be K full-length segments, where K is the largest integer for which $(K-1)R + (L-1) \leq Q-1$. The periodogram of the rth segment is

$$I_r(\omega) = \frac{1}{LU}|X_r(e^{j\omega})|^2, \tag{10.68}$$

where $X_r(e^{j\omega})$ is the discrete-time Fourier transform of $x_r[n]$. Each $I_r(\omega)$ has the properties of a periodogram, as described previously. Periodogram averaging consists of averaging together the K periodogram estimates $I_r(\omega)$; i.e., we form the time-averaged periodogram defined as

$$\bar{I}(\omega) = \frac{1}{K}\sum_{r=0}^{K-1} I_r(\omega). \tag{10.69}$$

To examine the bias and variance of $\bar{I}(\omega)$, let us take $L = R$, so that the segments do not overlap, and assume that $\phi_{xx}[m]$ is small for $m > L$; i.e., signal samples more than L apart are approximately uncorrelated. Then it is reasonable to assume that the periodograms $I_r(\omega)$ will be identically distributed independent random variables. Under this assumption, the expected value of $\bar{I}(\omega)$ is

$$\mathcal{E}\{\bar{I}(\omega)\} = \frac{1}{K}\sum_{r=0}^{K-1} \mathcal{E}\{I_r(\omega)\}, \tag{10.70}$$

or, since we assume that the periodograms are independent and identically distributed,

$$\mathcal{E}\{\bar{I}(\omega)\} = \mathcal{E}\{I_r(\omega)\} \qquad \text{for any } r. \tag{10.71}$$

From Eq. (10.61), it follows that

$$\mathcal{E}\{\bar{I}(\omega)\} = \mathcal{E}\{I_r(\omega)\} = \frac{1}{2\pi LU}\int_{-\pi}^{\pi} P_{xx}(\theta)C_{ww}(e^{j(\omega-\theta)})d\theta, \tag{10.72}$$

where L is the window length. When the window $w[n]$ is the rectangular window, the

method of averaging periodograms is called *Bartlett's procedure*, and in this case it can be shown that

$$c_{ww}[m] = \begin{cases} L - |m|, & |m| \leq (L-1), \\ 0 & \text{otherwise}, \end{cases} \tag{10.73}$$

and, therefore,

$$C_{ww}(e^{j\omega}) = \left(\frac{\sin(\omega L/2)}{\sin(\omega/2)} \right)^2. \tag{10.74}$$

That is, the expected value of the average periodogram spectrum estimate is the convolution of the true power spectrum with the Fourier transform of the triangular sequence $c_{ww}[n]$ that results as the autocorrelation of the rectangular window. Thus, the average periodogram is also a biased estimate of the power spectrum.

To examine the variance, we use the fact that, in general, the variance of the average of K independent identically distributed random variables is $1/K$ times the variance of each individual random variable. (See Papoulis, 1991.) Therefore, the variance of the average periodogram is

$$\text{var}[\bar{I}(\omega)] = \frac{1}{K} \text{var}[I_r(\omega)], \tag{10.75}$$

or, with Eq. (10.65), it follows that

$$\text{var}[\bar{I}(\omega)] \simeq \frac{1}{K} P_{xx}^2(\omega). \tag{10.76}$$

Consequently, the variance of $\bar{I}(\omega)$ is inversely proportional to the number of periodograms averaged, and as K increases, the variance approaches zero.

From Eq. (10.74), we see that as L, the length of the segment $x_r[n]$, increases, the main lobe of $C_{ww}(e^{j\omega})$ decreases in width, and consequently, from Eq. (10.72), $\mathcal{E}\{\bar{I}(\omega)\}$ more closely approximates $P_{xx}(\omega)$. However, for fixed total data length Q, the total number of segments (assuming that $L = R$) is Q/L; therefore, as L increases, K decreases. Correspondingly, from Eq. (10.76), the variance of $\bar{I}(\omega)$ will increase. Thus, as is typical in statistical estimation problems, for a fixed data length there is a trade-off between bias and variance. However, as the data length Q increases, both L and K can be allowed to increase, so that as Q approaches ∞, the bias and variance of $\bar{I}(\omega)$ can approach zero. Consequently, periodogram averaging provides an asymptotically unbiased, consistent estimate of $P_{xx}(\omega)$.

The preceding discussion assumed that nonoverlapping rectangular windows were used in computing the time-dependent periodograms. Welch (1970) showed that if a different window shape is used, the variance of the average periodogram still behaves as in Eq. (10.76). Welch also considered the case of overlapping windows and showed that if the overlap is one-half the window length, the variance is further reduced by almost a factor of 2, due to the doubling of the number of sections. Greater overlap does not continue to reduce the variance, because the segments become less and less independent as the overlap increases.

10.6.4 Computation of Average Periodograms Using the DFT

As with the periodogram, the average periodogram can be explicitly evaluated only at a discrete set of frequencies. Because of the availability of the fast Fourier transform algorithms for computing the DFT, a particularly convenient and widely used choice is the set of frequencies $\omega_k = 2\pi k/N$ for an appropriate choice of N. From Eq. (10.69), we see that if the DFT of $x_r[n]$ is substituted for the Fourier transform of $x_r[n]$ in Eq. (10.68), we obtain samples of $\bar{I}(\omega)$ at the DFT frequencies $\omega_k = 2\pi k/N$ for $k = 0, 1, \ldots, N-1$. Specifically, with $X_r[k]$ denoting the DFT of $x_r[n]$,

$$I_r[k] = I_r(\omega_k) = \frac{1}{LU}|X_r[k]|^2, \tag{10.77a}$$

$$\bar{I}[k] = \bar{I}(\omega_k) = \frac{1}{K}\sum_{r=0}^{K-1} I_r[k]. \tag{10.77b}$$

We denote $I_r(2\pi k/N)$ as the sequence $I_r[k]$ and $\bar{I}(2\pi k/N)$ as the sequence $\bar{I}[k]$. According to Eqs. (10.77a) and (10.77b), the average periodogram estimate of the power spectrum is computed at N equally spaced frequencies by averaging the DFTs of the windowed data segments with the normalizing factor LU. This method of power spectrum estimation provides a very convenient framework within which to trade between resolution and variance of the spectral estimate. It is particularly simple and efficient to implement using the fast Fourier transform algorithms discussed in Chapter 9. An important advantage of the method over those to be discussed in Section 10.7 is that the spectrum estimate is always nonnegative.

10.6.5 An Example of Periodogram Analysis

Power spectrum analysis is a valuable tool for modeling signals, and it also can be used to detect signals, particularly when it comes to finding hidden periodicities in sampled signals. As an example of this type of application of the average periodogram method, consider the sequence

$$x[n] = A\cos(\omega_0 n + \theta) + e[n], \tag{10.78}$$

where θ is a random variable uniformly distributed between 0 and 2π and $e[n]$ is a zero-mean white-noise sequence that has a constant power spectrum; i.e., $P_{ee}(\omega) = \sigma_e^2$ for all ω. In signal models of this form, the cosine is generally the desired component and $e[n]$ is an undesired noise component. Often, in practical signal detection problems we are interested in the case for which the power in the cosine signal is small compared with the noise power. It can be shown (see Problem 10.34) that over one period in frequency, the power spectrum for this signal is

$$P_{xx}(\omega) = \frac{A^2\pi}{2}[\delta(\omega - \omega_0) + \delta(\omega + \omega_0)] + \sigma_e^2 \qquad \text{for } |\omega| \le \pi. \tag{10.79}$$

From Eqs. (10.72) and (10.79), it follows that the expected value of the average periodogram is

$$\mathcal{E}\{\bar{I}(\omega)\} = \frac{A^2}{4LU}[C_{ww}(e^{j(\omega-\omega_0)}) + C_{ww}(e^{j(\omega+\omega_0)})] + \sigma_e^2. \tag{10.80}$$

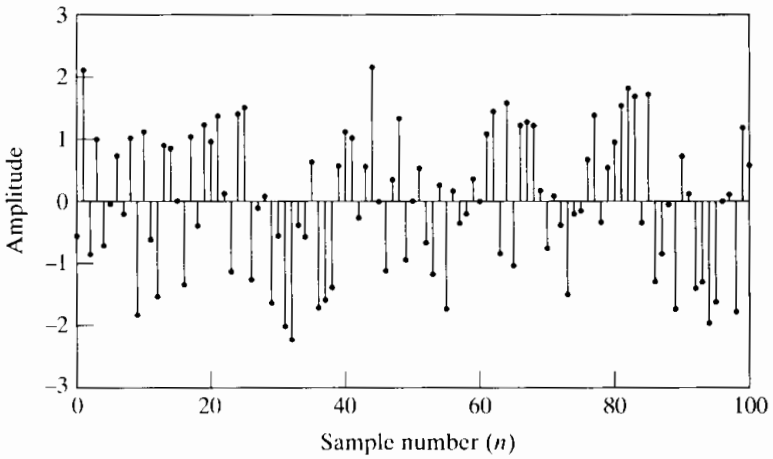

Figure 10.22 Cosine sequence with white noise, as in Eq. (10.78).

Figures 10.22 and 10.23 show the use of the averaging method for a signal of the form of Eq. (10.78), with $A = 0.5$, $\omega_0 = 2\pi/21$, and random phase $0 \leq \theta < 2\pi$. The noise was uniformly distributed in amplitude such that $-\sqrt{3} < e[n] \leq \sqrt{3}$. Therefore, it is easily shown that $\sigma_e^2 = 1$. The mean of the noise component is zero. Figure 10.22 shows 101 samples of the sequence $x[n]$. Since the noise component $e[n]$ has maximum amplitude $\sqrt{3}$, the cosine component in the sequence $x[n]$ is not visually apparent.

Figure 10.23 shows average periodogram estimates of the power spectrum for rectangular windows with amplitude 1, so that $U = 1$, and of lengths $L = 1024$, 256, 64, and 16, with the total record length $Q = 1024$ in all cases. Except for Figure 10.23(a), the windows overlap by one-half the window length. Figure 10.23(a) is the periodogram of the entire record, and Figures 10.23(b), (c), and (d) show the average periodogram for $K = 7$, 31, and 127 segments, respectively. In all cases, the average periodogram was evaluated using 1024-point DFTs at frequencies $\omega_k = 2\pi k/1024$. (For window lengths $L < 1024$, we must pad the windowed sequence with zero-samples before computing the DFT.) Therefore, the frequency $\omega_0 = 2\pi/21$ lies between DFT frequencies $\omega_{48} = 2\pi 48/1024$ and $\omega_{49} = 2\pi 49/1024$.

In using such estimates of the power spectrum to detect the presence and/or the frequency of the cosine component, we might search for the highest peaks in the spectral estimate and compare their size with that of the surrounding spectral values. From Eqs. (10.74) and (10.80), the expected value of the average periodogram at the frequency ω_0 is

$$\mathcal{E}\{\bar{I}(\omega_0)\} = \frac{A^2 L}{4} + \sigma_e^2. \tag{10.81}$$

Thus, if the peak due to the cosine component is to stand out against the variability of the average periodogram, then in this special case we must choose L so that $A^2 L/4 \gg \sigma_e^2$. This is illustrated by Figure 10.23(a), where L is as large as it can be for the record length Q. We see that $L = 1024$ gives a very narrow main lobe of the Fourier transform of the autocorrelation of the rectangular window, so it would be possible to resolve very closely spaced sinusoidal signals. Note that for the parameters of this example ($A = 0.5$, $\sigma_e^2 = 1$) and with $L = 1024$, the peak amplitude in the periodogram at frequency $2\pi/21$ is close, but not equal, to the expected value of 65. We also observe additional peaks in the periodogram with amplitudes greater than 10. Clearly, if the cosine amplitude A had been smaller by only a factor of 2, it is possible that its peak would have been confused with the inherent variability of the periodogram.

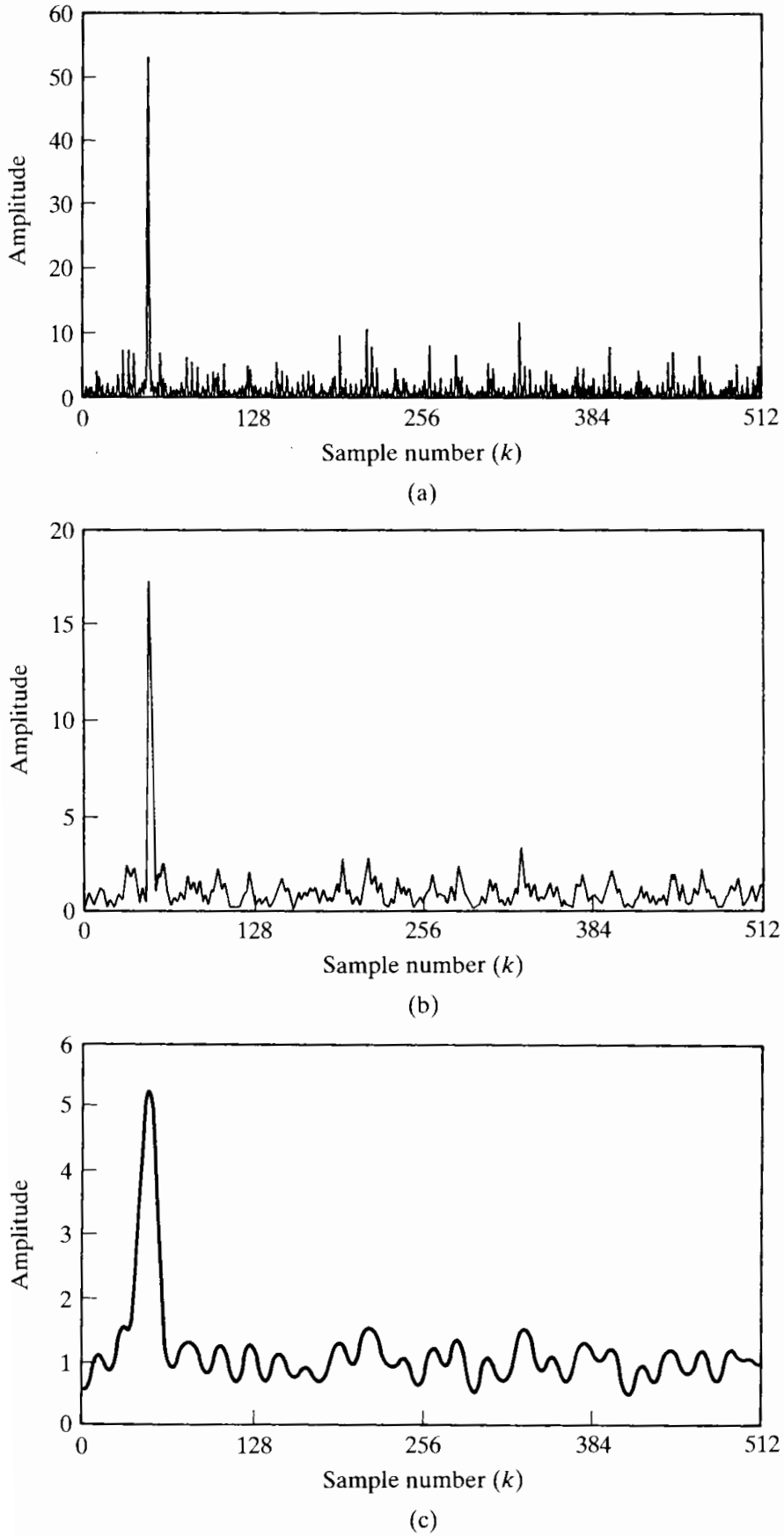

Figure 10.23 Example of average periodogram for signal of length $Q = 1024$. (a) Periodogram for window length $L = Q = 1024$ (only one segment). (b) $K = 7$ and $L = 256$ (overlap by $L/2$). (c) $K = 31$ and $L = 64$.

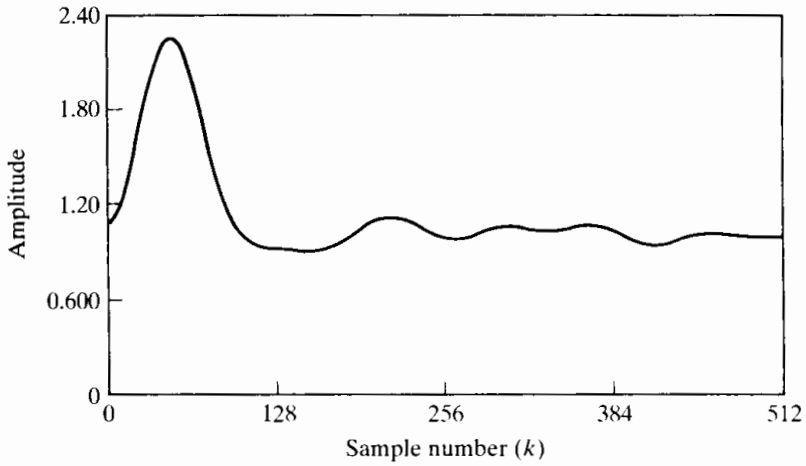

(d)

Figure 10.23 (*continued*) (d) $K = 127$ and $L = 16$.

We have seen that the only sure way to reduce the variance of the spectrum estimate is to increase the record length of the signal. This is not always possible, and even if it is possible, longer records require more processing. We can reduce the variability of the estimate while keeping the record length constant if we use shorter windows and average over more sections. The cost of doing this is illustrated by parts (b), (c), and (d) of Figure 10.23. Note that as more sections are used, the variance of the spectral estimate decreases, but in accordance with Eq. (10.81), so does the amplitude of the peak due to the cosine. Thus, we again face a trade-off. That the shorter windows reduce variability is clear, especially if we compare the high-frequency regions away from the peak in parts (a), (b) and (c) of Figure 10.23. Recall that the idealized power spectrum of the model for the pseudorandom-noise generator is a constant ($\sigma_e^2 = 1$) for all frequencies. In Figure 10.23(a) there are peaks as high as about 10 when the true spectrum is 1. In Figure 10.23(b) the variation away from 1 is less than about 3, and in Figure 10.23(c) the variation around 1 is less than .5. However, shorter windows also reduce the peak amplitude of any narrowband component, and they also degrade our ability to resolve closely spaced sinusoids. This reduction in peak amplitude is also clear from Figure 10.23. Again, if we were to reduce A by a factor of 2 in Figure 10.23(b), the peak height would be approximately 4, which is not much different from many of the other peaks in the high-frequency region. In Figure 10.23(c) a reduction of A by a factor of 2 would make the peak approximately 1.25, which would be indistinguishable from the other ripples in the estimate. In Figure 10.23(d) the window is very short, and thus the fluctuations of the spectrum estimate are greatly reduced, but the spectral peak due to the cosine is very broad and barely above the noise even for $A = .5$. If the length were any smaller, spectral leakage from the negative-frequency component would cause there to be no distinct peak in the low-frequency region.

This example confirms that the average periodogram provides a straightforward method of trading off between spectral resolution and reduction of the variance of the spectral estimate. Although the theme of the example was the detection of a sinusoid in noise, the average periodogram could also be used in signal modeling. The spectral estimates of Figure 10.23 clearly suggest a signal model of the form of Eq. (10.78), and most of the parameters of the model could be estimated from the average periodogram power spectrum estimate.